Journal of Experimental Botany
doi:10.1093/jxb/eru464

Journal of Experimental Botany
www.jxb.oxfordjournals.org

RESEARCH PAPER

Role of AtMSH7 in UV-B-induced DNA damage recognition and recombination

Luciana Daniela Lario[1,*], Pablo Botta[1,†], Paula Casati[1,‡] and Claudia Patricia Spampinato[1,‡]

[1] Centro de Estudios Fotosintéticos y Bioquímicos (CEFOBI), Facultad de Ciencias Bioquímicas y Farmacéuticas, Universidad Nacional de Rosario, Suipacha 531, 2000 Rosario, Argentina

* Present address: Department of Biochemical and Pharmaceutical Technology, University of São Paulo, 05508-000 São Paulo, Brazil
† Present address: Biotechnology Department, Nidera S.A., Ruta 8 Km 376, 2600 Venado Tuerto, Santa Fe, Argentina
‡ To whom correspondence should be addressed. E-mail: casati@cefobi-conicet.gov.ar (PC); spampinato@cefobi-conicet.gov.ar (CPS)

Received 24 July 2014; Revised 6 October 2014; Accepted 21 October 2014

Abstract

The mismatch repair (MMR) system maintains genome integrity by correcting replication-associated errors and inhibiting recombination between divergent DNA sequences. The basic features of the pathway have been highly conserved throughout evolution, although the nature and number of the proteins involved in this DNA repair system vary among organisms. Plants have an extra mismatch recognition protein, MutSγ, which is a heterodimer: MSH2–MSH7. To further understand the role of MSH7 *in vivo*, we present data from this protein in *Arabidopsis thaliana*. First, we generated transgenic plants that express β-glucuronidase (GUS) under the control of the *MSH7* promoter. Histochemical staining of the transgenic plants indicated that *MSH7* is preferentially expressed in proliferating tissues. Then, we identified *msh7* T-DNA insertion mutants. Plants deficient in MSH7 show increased levels of UV-B-induced cyclobutane pyrimidine dimers relative to wild-type (WT) plants. Consistent with the patterns of MSH7 expression, we next analysed the role of the protein during somatic and meiotic recombination. The frequency of somatic recombination between homologous or homeologous repeats (divergence level of 1.6%) was monitored using a previously described GUS recombination reporter assay. Disruption of *MSH7* has no effect on the rates of somatic homologous or homeologous recombination under control conditions or after UV-B exposure. However, the rate of meiotic recombination between two genetically linked seed-specific fluorescent markers was 97% higher in *msh7* than in WT plants. Taken together, these results suggest that *MSH7* is involved in UV-B-induced DNA damage recognition and in controlling meiotic recombination.

Key words: *Arabidopsis thaliana*, meiotic recombination, mismatch repair, mitotic recombination, sequence divergence, UV-B radiation.

Introduction

The mismatch repair (MMR) system is a highly conserved DNA repair pathway essential for the correct maintenance of genetic information across generations (reviewed in Kunkel and Erie, 2005; Iyer *et al.*, 2006; Jiricny, 2006; Hsieh and Yamane, 2008; Li, 2008). The pathway is best known for its role in the correction of single base–base mismatches and unpaired nucleotides in nascent or template DNA strands [insertion or deletion loops (IDLs), respectively] which have arisen through replication errors, deamination of 5-methylcytosine, and recombination between divergent sequences. The MMR system is also associated with processing and/or signalling of different types of DNA damage (reviewed in Iyer *et al.*, 2006; Jiricny, 2006; Hsieh and Yamane, 2008; Li, 2008).

The repair pathway functions through complex interactions among multiple proteins, which have been conserved from bacteria to plants (Spampinato *et al.*, 2009). In eukaryotes, the initial recognition of DNA lesions is carried out by heterodimer complexes known as MutSα (MSH2–MSH6) and MutSβ (MSH2–MSH3). MutSα recognizes base–base mismatches and single IDLs, while MutSβ mainly binds IDLs of 2–12 bases (Acharya *et al.*, 1996; Genschel *et al.*, 1998). In addition, plants contain a unique MutS protein, MutSγ (MSH2–MSH7) (Ade *et al.*, 1999; Horwath *et al.*, 2002; Tam *et al.*, 2009). At present, MutSγ has been characterized to a more limited extent than MutSα and MutSβ. Previous studies have suggested that MutSγ preferentially recognizes certain base–base mismatches (Culligan and Hays, 2000; Wu *et al.*, 2003). Interestingly, functional analyses in yeast have demonstrated that MutSγ is important in recognizing local sequence environments containing T and/or G/T, A/C, T/C, G/A, T/T, or A/A mismatches which have arisen by deamination of cytosine and 5-methylcytosine, and by UV or oxidative mutagenesis (Gomez and Spampinato, 2013). In addition, it was suggested that MSH7 has an important function during meiosis. Support for this hypothesis has come from the following observations: (i) in wheat (*Triticum aestivum*), *MSH7* is highly expressed in the reproductive organs of young flower spikes and was mapped to a locus, termed *Ph2*, known to affect homoeologous recombination (Dong *et al.*, 2002); (ii) in transgenic barley (*Hordeum vulgare*), the expression of MSH7 was required for plant fertility (Lloyd *et al.*, 2007); and (iii) in tomato (*Solanum lycopersicum*), suppression of *MSH7* by gene silencing was associated with a modest increase in recombination between tomato and its distant wild relative *Solanum lycopersicoides* as determined by PCR-based cleaved amplified polymorphic sequence and simple sequence repeat markers (Tam *et al.*, 2011).

To further understand the role of MSH7 *in vivo*, we present data that demonstrates its participation in UV-B-induced DNA damage recognition and in meiotic recombination in *Arabidopsis thaliana*. First, we analysed the localization of MSH7 *in vivo*, showing that the protein is mainly expressed in proliferative tissues. We then studied the role of the protein *in vivo* by analysis of *msh7* mutant lines maintained under control conditions or exposed to UV-B radiation. UV-B radiation induces the formation of covalent bonds between adjacent pyrimidine residues along a DNA strand giving rise to cyclobutane pyrimidine dimers (CPDs) and, to a lesser extent, pyrimidine (6-4) pyrimidone photoproducts. Previous results performed in our laboratory provide evidence that plant MSH2 and MSH6 are involved in a UV-B-induced DNA damage response pathway (Lario *et al.*, 2011). In this work, we extend these observations and show that *msh7* plants are less efficient at removing UV-B-induced CPDs relative to wild-type (WT) plants. In addition, we demonstrate that the *msh7* mutation does not affect the rates of somatic homologous or homeologous recombination under control conditions or after UV-B exposure, but influences the rates of meiotic recombination between two genetically linked seed-specific fluorescent markers.

Materials and methods

Plant material and growth conditions

Arabidopsis WT and *msh7* T-DNA insertion lines (SALK_031214 and CS855482) were sown directly on soil and placed at 4°C in the dark. After 3 days, pots were transferred to a greenhouse and plants were grown at 22°C under a 16h/8h light/dark regime. The T-DNA insertion lines were obtained from the *Arabidopsis* SALK collection (Alonso *et al.*, 2003) at the Arabidopsis Biological Resource Center (ABRC, Columbus, OH, USA). All lines are in the Columbia background. In every experiment, WT plants were grown together with *msh7* mutants to avoid variability in environmental conditions.

Expression analysis and GUS staining

A 592-bp region containing the At*MSH7* promoter was amplified by PCR using LP-HindIII-pM7 and RP-XbaI-pM7 primers (Supplementary Table S1). The amplification product was fused to the β-glucuronidase (GUS) reporter gene (*uidA*) in pBI101.1 vectors (Jefferson, 1987). This pMSH7:GUS fusion construct was transformed in *Arabidopsis* (Columbia ecotype) plants using *Agrobacterium tumefaciens* C58CRifR by the floral dip method (Clough and Bent, 1998). Transformed seedlings (T0 generation) were selected on Murashige and Skoog agar plates containing 50 mg ml^{-1} kanamycin and transferred to soil. T2 homozygous plants were selected for further analysis. Histochemical detection of GUS activity was carried out using 5-bromo-4-chloro-3-indolyl-β-D-glucuronide (X-gluc) (Jefferson, 1987). GUS-stained tissues shown here represent typical results of at least three independent transient transformation lines.

Identification of insertional T-DNA mutants

The initial screening of *Arabidopsis* T-DNA insertion lines was performed by a PCR-based approach using genomic DNA isolated from leaves by a modified cetyltrimethylammonium bromide (CTAB) method (Sambrook and Russel, 2001) and three combinations of primers (Supplementary Table S1). Two primers hybridize to specific genomic sequences (LP-31214 and RP-31214 for the SALK_031214 line; and LP-855482 and RP-855482 for the CS855482 line) and one primer is located inside the left border of the T-DNA (LB-SALK). The presence or absence of the T-DNA insertion in the genes allowed the identification of homozygous, heterozygous, and WT plants.

Homozygous lines were further analysed by quantitative real-time PCR (qRT-PCR) to confirm the absence of the *MSH7* transcript (Supplementary Figure S1). Total RNA was isolated from about 100 mg of seedlings using the TRIzol reagent (Invitrogen) as described in the manufacturer's protocol. All RNA samples were incubated with RNase-free DNase I (1 U ml^{-1}) to remove traces of genomic DNA. Reverse transcription was performed with 4 μg of RNA using SuperScript II reverse transcriptase (Invitrogen) and oligo-dT as a primer. The resultant cDNA was used as a template for qRT-PCR amplification in a MiniOPTICON2 apparatus (Bio-Rad) with specific primers (LP-M7 and RP-M7; Supplementary Table S1) spanning a 231-bp region of AtMSH7 cDNA, Platinum Taq DNA Polymerase (Invitrogen), and the intercalation dye SYBRGreen I (Invitrogen) as the fluorescent reporter. Gene expression was normalized to the *Arabidopsis* translation elongation factor EF1A (Supplementary Table S1).

UV-B irradiation of plants

Arabidopsis plants were exposed to UV-B radiation during 4 h in a growth chamber. UV-B lamps (Bio-Rad, Hercules, California) were covered with cellulose acetate filters (100 μm extra clear cellulose acetate plastic; Tap Plastics, Mountain View, CA, USA) and placed 30 cm above the plants. The cellulose acetate sheeting excludes wavelengths lower than 280 nm, but does not remove any

UV-B radiation from the spectrum. The UV radiation intensities measured with a UV-B/UV-A radiometer (UV203 AB radiometer; Macam Photometrics, UK) were 2 W m^{-2} and 0.65 W m^{-2} for UV-B and UV-A, respectively. Control plants without supplementary UV-B radiation were exposed for the same period of time to light sources described above covered with cellulose acetate and polyester filters (100 µm clear polyester plastic; Tap Plastics, Mountain View, CA, USA). This polyester filter absorbs both UV-B (0.04 W m^{-2}) and wavelengths lower than 280 nm. The UV-A radiation intensity was 0.4 W m^{-2}.

DNA damage analysis

After UV-B treatment, seedlings (100 mg) from at least three independent biological replicates were collected, frozen in liquid nitrogen and stored at –80°C. Induction of CPDs was determined by a previously described assay (Stapleton *et al.*, 1993). Briefly, 1.5 µg of the extracted DNA was denatured in 0.3 M NaOH for 10 min and 6-fold dot blotted onto a nylon membrane (Hybond N+, GE Healthcare Life Sciences). The membrane was blocked in TBS (20 mM Tris-HCl, pH 7.6, 137 mM NaCl) containing 5% dried milk for 1 h at room temperature. The blot was then washed and incubated with a 1:2000 dilution of monoclonal antibodies specific to CPDs (TDM-2, Cosmo Bio Co., Ltd, Japan) for 16 h at 4°C with agitation. Unbound antibodies were washed away and a dilution of 1:3000 of secondary antibodies conjugated to alkaline phosphatase (BioRad) was added. The blot was then washed several times followed by the addition of 5-bromo-4-chloro-3-indolyl phosphate and nitroblue tetrazolium. Quantification was achieved by densitometry of the dot blot using ImageQuant software version 5.2. The amount of CPDs was normalized to the amount of DNA run on 1% (w/v) agarose gels after quantification.

Intrachromosomal recombination experiments and GUS staining

Homozygous *msh7* (CS855482) plants were crossed with WT plants transformed with A0 or A10 constructs (Opperman *et al.*, 2004) using *A. tumefaciens* as described above. A0 and A10 lines contain two overlapping halves of the GUS reporter gene (namely GU and US) separated by the *NPTII* (neomycin phosphotransferase) gene spacer. U repeats (618 bp) display sequence identities (A0) or contain ten mismatches (A10) between them. F2 plants were obtained and the GUS reporter gene was monitored in these plants by PCR using LP-GUS and RP-GUS primers (Supplementary Table S1). Seeds expressing the A0 or A10 construct which were *MSH7*/*MSH7* or *msh7*/*msh7* homozygous were selected, stratified at 4°C for 3 days, and grown for 3 weeks. Seedlings were then exposed to UV-B radiation or maintained under control conditions during 4 h in a growth chamber as described above and grown for another week in the absence of UV-B. Plants were then harvested and incubated in staining solution containing X-gluc. Blue sectors expressing the restored GUS gene were counted under a microscope.

Meiotic recombination

Homozygous *msh7* (CS855482) plants were crossed with the previously described Columbia background meiotic tester line Col3-4/20 (Melamed-Bessudo *et al.*, 2005). This tester line contains two reporter genes that encode green (GFP) and red (RFP) fluorescent proteins located on chromosome 3 at a physical distance of 5.1 Mb and a genetic distance of 16 cM, and are driven by a seed-specific promoter. Fluorescent markers were monitored in the self-progeny (F2) of these plants by PCR using the TAIL primer specific for the left border of the T-DNA and GCo39 or RCo39 (green or red insertion, respectively) primers (Supplementary Table S1). Seeds expressing both GFP and RFP markers and being *MSH7*/*MSH7* or *msh7*/*msh7* were selected. Seeds from these plants with exclusively green or red fluorescence indicate a meiotic recombination event between the markers. The recombination rate (r) was calculated using the following equation:

$$r = \frac{2 - \sqrt{4 - \left[4 \times 2 \times (G+R)/N\right]}}{2}$$

where G is the number of green-only seeds, R is the number of red-only seeds, and N is the total number of seeds (Melamed-Bessudo *et al.*, 2005). Seed fluorescence was evaluated using a Zeiss Axiovert 25 CFL microscope equipped with GFP- and RFP-specific filters and an Olympus Q-Colour 5 camera. Fluorescence was then analysed using Image-Pro Plus software.

Results

MSH7 is expressed in actively dividing cells

To study the spatial and temporal expression of MSH7, we fused a 592-bp fragment of the *MSH7* promoter to the GUS reporter gene and transformed the resulting construct (*pMSH7:GUS*) into WT Col0 plants. At least three independent transgenic lines with comparable GUS activity levels were analysed. GUS staining was detected at high levels in shoot and root apical regions (Fig. 1A). In 10-day-old seedlings, *MSH7* was restricted to the shoot and root apical meristems, and proliferating leaves (Fig. 1B), while *MSH7* expression was undetectable in mature leaves. The same pattern was observed in 20-day-old plants (Fig. 1C). Interestingly, *MSH7* was clearly restricted to the lower half of the leaf (Fig. 1D), consistent with a gradient of mitotic activity along the proximal-distal axis (Donnelly *et al.*, 1999). In roots, *MSH7* was localized in root tips, coinciding with root apical meristems where active cell divisions take place (Fig. 1E).

GUS expression was also detected in unopened flower buds and mature flowers (Fig. 1F–H). The expression pattern was restricted to the pistil (Fig. 1H). We did not observe any GUS expression in anthers or in pollen on the stigmatic surface (Fig. 1H). Developing seeds also showed GUS staining (Fig. 1I). These results indicate that *MSH7* is highly expressed in actively dividing tissues.

Functional role of MSH7 protein in the repair of UV-B-damaged DNA

Previously, we demonstrated that both *Arabidopsis* MSH2 and MSH6 proteins participate in UV-B-induced DNA damage repair (Lario *et al.*, 2011). Therefore, the role of the MSH7 protein in the repair of UV-B-induced DNA lesions was also analysed using two independent T-DNA insertional lines, SALK_031214 and CS855482, with insertions in the fourth and 12th introns, respectively. Insertional inactivation of *MSH7* was confirmed by qRT-PCR (Supplementary Figure S1). None of the described mutants showed any visible phenotype under standard growth chamber conditions in the first and second generations, as previously described for *msh2* and *msh6* mutants (Hoffman *et al.*, 2004; Lario *et al.*, 2011).

To test the hypothesis that MSH7 can also contribute to UV-B-induced DNA repair *in vivo*, *Arabidopsis* WT plants and *msh7* mutants were grown in a growth chamber in the absence of UV-B for 3 weeks. Then, plants were exposed for 4 h under UV-B radiation (2 W.m^{-2}). As a control, different

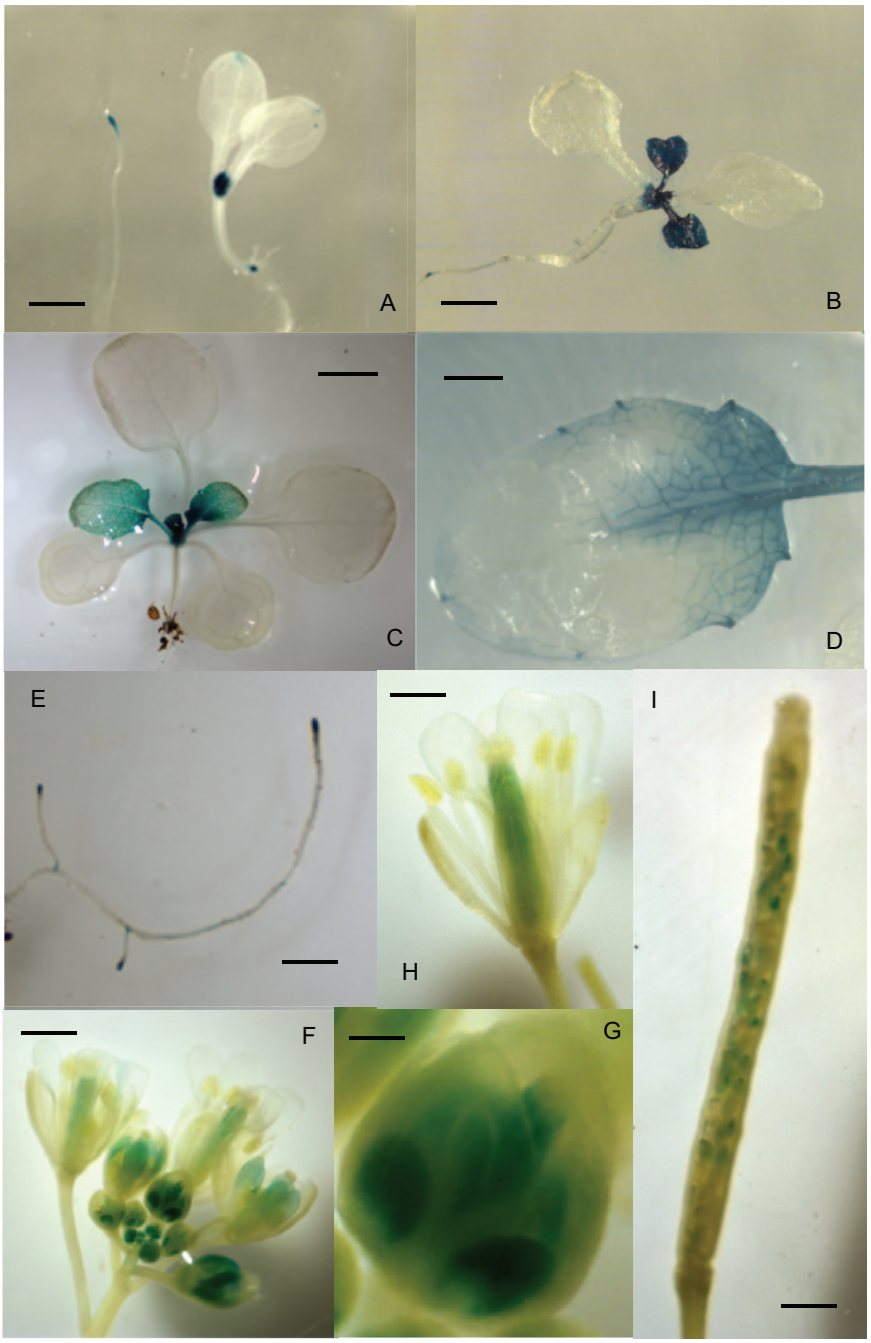

Fig. 1. Histochemical analysis of GUS activity in transgenic *Arabidopsis* plants transformed with the pMSH7:GUS construct. (A) Seedlings 5 days after germination. Bar: 1 mm. (B) Ten-day-old whole seedlings. Bar: 1 mm. (C) Twenty-day-old whole seedlings. Bar: 2 mm. (D) Close-up of an expanded leaf. Bar: 0.4 mm. (E) Roots. Bar: 1 mm. (F) Flowers at different stages of development. Bar: 1 mm. (G) Unopened flower bud. Bar: 0.15 mm. (H) Mature flower. Bar: 0.5 mm. (I) Siliques. Bar: 1 mm. This figure is available in colour at *JXB* online.

sets of plants were irradiated with the same lamps covered with a polyester plastic that absorbs UV-B. Leaf samples from control and treated plants were collected immediately after the end of the UV-B treatment. DNA was extracted and the CPD abundance was determined in each mutant and compared to that in WT plants. In the absence of UV-B, the steady-state levels of CPDs in WT and *msh7* mutants were similar [100 optical density (IOD) in all samples]. However, after 4 h of exposure to UV-B radiation, small but statistically significant increases of unrepaired lesions were detected in SALK_031214 (39.6%) and CS855482 (14.5%) compared to WT plants (Fig. 2). These results suggest that MSH7 contributes to UV-B-induced DNA damage recognition, as similarly reported for MSH2 and MSH6 (Lario *et al.*, 2011).

MSH7 does not affect somatic recombination

Somatic recombination was monitored in WT and *msh7* mutant (CS855482) plants crossed with A0 and A10 constructs (Opperman *et al.*, 2004). These constructs contain two overlapping fragments of the GUS reporter gene which display sequence identities (A0) or contain ten mismatches (A10)

between them. Thereby, the number of blue sectors in which the functional GUS gene is restored is indicative of the frequencies of somatic recombination. Table 1 shows that statistically similar recombination frequencies in the absence of mismatches (homologous recombination) were observed for the WT (1.75 ± 0.46) and *msh7* mutant (1.67 ± 0.53) maintained under control conditions. These frequencies were significantly reduced ($P < 0.01$) in the presence of mismatches (homeologous recombination), although to the same extents in the WT (0.058 ± 0.056) and *msh7* mutant (0.033 ± 0.043). Similar analyses were carried out after exposure of the plantlets with UV-B radiation to test whether this radiation affects recombination rates in both or either plants. No significant differences in the number of recombination events per plant were observed in the absence (1.57 ± 0.48 and 2.30 ± 0.78 for the WT and *msh7* mutant, respectively) or presence (0.033 ± 0.043 and 0.042 ± 0.044 for the WT and *msh7* mutant, respectively) of mismatches. These results show that MSH7 is not essential for somatic homologous or homeologous recombination.

Enhanced meiotic recombination rates in the msh7 mutant

To gain insight into the role of MSH7 in meiotic recombination, the homozygous tester line Col3-4/20 in a background of the ecotype Columbia (Melamed-Bessudo *et al.*, 2005) was crossed with the *msh7* mutant (CS855482). The tester line contains both RFP and GFP markers, under the seed-specific *NapA* promoter, located on chromosome 3 at physical and genetic distances of 5.1 Mb and 16 cM, respectively. Therefore, this line allows estimation of meiotic recombination rates by counting seeds expressing both (red and green), only one (red or green), or neither fluorescent marker. Crossover rates between the markers were 16.2 cM in *MSH7*/*MSH7* plants (Table 2), not significantly different from previously published values (16.3, 16.4, and 15.4 cM) (Melamed-Bessudo *et al.*, 2005; Pecinka *et al.*, 2011; Melamed-Bessudo and Levy, 2012). The *msh7* mutation led to meiotic recombination rates of 31.9 cM (Table 2), an increase of 97% compared to the WT ($P < 0.01$, analysed by unpaired Student's *t*- test). These results indicate that MSH7 affects meiotic recombination.

Discussion

Differential expression of MSH7 in mitotic and meiotic tissues

Previous reports have analysed the expression pattern of *MSH7* from *T. aestivum* and *S. lycopersicum* by northern hybridization (Dong *et al.*, 2002) and semi-quantitative RT-PCR (Tam *et al.*, 2009), respectively. The highest expression of *MSH7* was detected in young flowers (Dong *et al.*, 2002; Tam *et al.*, 2009), young leaves (Tam *et al.*, 2009), and young flower spikes (Dong *et al.*, 2002). We have confirmed

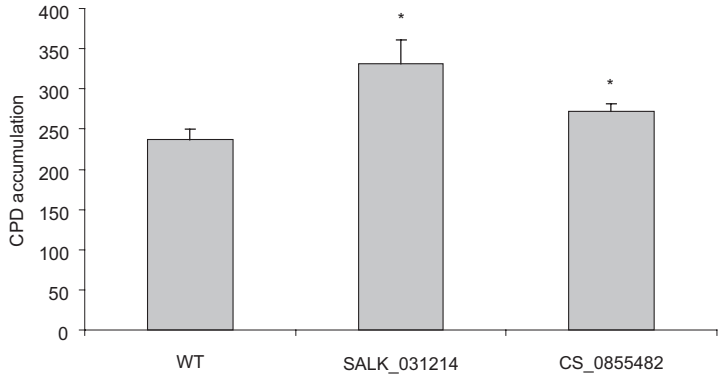

Fig. 2. CPD levels in DNA extracted from WT, SALK_031214, and CS855482 plants exposed to 4 h UV-B radiation relative to control conditions. CPDs were quantified by an immunological sensitive assay. Results represent the average ± SD of three independent biological replicates. Asterisks denote statistical differences applying the Student's *t*-test ($P < 0.05$).

Table 1. *Recombination frequency between identical (A0) and divergent (A10) sequences in WT (MSH7/MSH7) or* msh7 *mutant background (msh7/msh7, CS855482 line)*[a]

Cross	Total seedlings	Recombination events		Recombination frequency	
		Control	UV-B	Control	UV-B
A0 × WT	140	123	110	1.75[b]	1.57[b]
A10 × WT	240	7	4	0.058[c]	0.033[c]
A0 × *msh7*	140	117	161	1.67[b]	2.30[b]
A10 × *msh7*	240	4	5	0.033[c]	0.042[c]

[a] Transgenic seedlings (140 or 240 depending on the construct) were grown for 3 weeks. Half of the seedlings were then exposed to UV-B radiation while the others were maintained under control conditions. All the seedlings were grown for another week in the absence of UV-B before histochemical detection of GUS activity. The recombination frequency is expressed as the average number of blue sectors per seedling. Statistical analysis between the different groups was carried out using the Wilcoxon test for non-parametric variables. Results with different letters are significantly different ($P < 0.01$).

Table 2. *Meiotic recombination rates between green and red fluorescent markers in F2 seeds of crosses between tester line Col3-4/20 × WT (MSH7/MSH7) or Col3-4/0 ×* msh7 *mutant background (msh7/msh7, CS855482 line)*[a]

Cross	Seeds	Seed fluorescence				Genetic distance (cM)
		Green only	Red only	Red and green	None	
Col3-4/20 × WT	2320	168	178	1475	500	16.2[b]
Col3-4/20 × *msh7*	1649	240	202	911	294	31.9[c]

[a] For each genotype, seeds derived from five individual plants were pooled and data were used to calculate mean recombination rates and *P* values using the unpaired Student's *t*-test. Results with different letters are significantly different ($P < 0.01$).

and extended these observations in more detail in *Arabidopsis* plants. We constructed transgenic plants expressing the GUS reporter gene directed by the At*MSH7* promoter. Our results validate that At*MSH7* is localized in root tips, shoot apical meristems, immature and mature flowers, and siliques (Fig. 1). We have also demonstrated that the protein expression is clearly associated with the mitotic activity of developing leaves and with developing seeds of young siliques (Fig. 1). These expression patterns indicate that At*MSH7* is largely confined to developing and meiotic tissues.

Role of MSH7 in CPD recognition and repair

We previously demonstrated that mutations in *MSH2* or *MSH6* caused an increased accumulation of CPDs relative to WT plants, providing evidence that plant MutSα is involved in a UV-B-induced DNA damage response pathway (Lario *et al.*, 2011). Similarly, elucidation of the role of AtMutSγ in UV-B-induced DNA damage recognition was performed using *msh7* mutant plants. The study was restricted to the analysis of CPD levels immediately after UV-B exposure by an immunological approach. Disruption of MSH7 caused an increased accumulation of CPDs relative to the WT (Fig. 2). Interestingly, recent research findings in our laboratory determined that AtMutSγ could be the protein which recognizes local sequence environments containing T and/or mismatches induced by UV light at cytosine-containing photoproducts or TT sequences, among other causes (Gomez and Spampinato, 2013).

MSH7 is not required in somatic recombination

Given that UV-B induces multiple forms of DNA damage (Pfeifer *et al.*, 2005) and that interconnections between MMR and recombination repair pathways exist (Emmanuel *et al.*, 2006; Li *et al.*, 2006; Lafleuriel *et al.*, 2007), we tested the effect of UV-B on the level of mitotic recombination and the direct involvement of MSH7 in the process. The frequencies of recombination were measured in the WT and the *msh7* mutant one week after UV-B exposure with GUS reporter recombination substrates (Opperman *et al.*, 2004) displaying sequence identities (homologous recombination) or containing 10 mismatches (divergence level of 1.62%) within the overlap (Table 1). We show that UV-B radiation does not alter the frequency of homologous recombination in WT plants. Previous studies suggested that treatment of plants with UV-B led to an increased rate of homologous recombination (Ries *et al.*, 2000*a*; Ries *et al.*, 2000*b*). Although this might suggest distinct results, the observations may reflect differences in study designs. It should also be noted that induction of recombination by UV-B observed by these previous studies correlated with UV-B regimes, levels of DNA damage, and light conditions applied to plants after exposure to UV radiation (Ries *et al.*, 2000*a*; Ries *et al.*, 2000*b*). These authors also show a drastic increase of recombination events in photolyase-deficient mutant plants (Ries *et al.*, 2000*a*). Indeed, our results agree with these observations because we measured recombination rates one week after UV-B exposure. Lack of a delayed hyperrecombination response with acute UV-B exposure was also observed in human cells (Durant *et al.*, 2006). Disruption of *MSH7* does not alter the frequency of homologous recombination under control conditions compared to WT plants as previously reported for *msh2* mutant plants (Emmanuel *et al.*, 2006). After UV-B irradiation of *msh7* plants, we found no induction of homologous recombination compared with control plants, confirming the minor contribution of MSH7 in CPD recognition and the important role of photolyases in monomerizing CPDs. In fact, the lack of CPD-specific photolyase repair with the concomitant prolonged persistence of this type of DNA damage in the genome has been reported to strongly influence the recombination process in plants (Ries *et al.*, 2000*a*).

Small heterologies within the recombination repeats decreased the frequency of recombination in WT plants under control conditions as previously observed (Li *et al.*, 2004; Opperman *et al.*, 2004; Emmanuel *et al.*, 2006). Assuming that MSH7 is able to specifically recognize G/T, A/C, T/C, G/A, T/T, and A/A mismatches (Gomez and Spampinato, 2013), and seven of these mismatches are found among the ten sequence differences of the heteroduplex intermediate (Opperman *et al.*, 2004), one would expect that homeologous recombination increased upon mutation of MSH7, but this was not observed. Inactivation of MSH7 leads to a similar drop-off in recombination rates as reported for WT plants, confirming that the MMR system is still functional due to the activity of MutSα (Culligan and Hays, 2000; Wu *et al.*, 2003). Note that plants defective for MSH2, MLH1, or PMS1 result in the loss of mismatch correction and show a higher frequency of homeologous recombination during somatic recombination (Emmanuel *et al.*, 2006; Li *et al.*, 2006; Dion *et al.*, 2007; Li *et al.*, 2009). We also demonstrate that acute UV-B exposure has no effect on the low frequencies of homeologous recombination in WT and *msh7* mutant plants.

Role of MSH7 in meiotic recombination

Previous reports suggested that MSH7 has a specialized role in meiotic recombination due to the early expression of *MSH7* from *T. aestivum* during meiosis and its linkage to the *Ph2* locus (Dong *et al.*, 2002), the reduced fertility of barley plants transformed with an *MSH7* RNAi knock-down construct (Lloyd *et al.*, 2007), and a modest increase in homeologous recombination in the *MSH7*-impaired line of *S. lycopersicum*, heterozygous for chromosome 8 from *S. lycopersicoides* (Tam *et al.*, 2011). Here, we used the previously described seed meiotic reporter line Col3-4/20, in the Columbia background, (Melamed-Bessudo *et al.*, 2005) to better understand the effect of AtMSH7 during meiotic recombination. During meiotic recombination, a single round of DNA replication is followed by two rounds of nuclear division. In the first division, homologous chromosomes segregate. Accurate segregation is ensured by the formation of at least one obligate crossover event per chromosome. In the second division, sister chromatids segregate and four haploid gametes are generated (Osman *et al.*, 2011). Meiosis in *Arabidopsis* and possibly other plants proceeds to its end point despite gross defects due to the lack of meiotic checkpoints (Caryl *et al.*, 2003). The recombination process is initiated by the formation of programmed double-strand breaks (DSBs) catalysed by SPO11 (Osman *et al.*, 2011). DSBs are subsequently repaired and crossovers or noncrossovers can be recovered. The formation of crossovers is regulated by many meiotic proteins which are classified as having either pro- or anti-crossover activities (Youds and Boulton, 2011). MSH4 and MSH5 were the first proteins to be implicated specifically in promoting crossover without having mismatch repair activity (Hoffmann and Borts, 2004). Homologues of MSH4 and MSH5 from *Arabidopsis* have been identified and characterized (Higgins *et al.*, 2004; Higgins *et al.*, 2008). Loss of these proteins results in a profound reduction in crossovers (Higgins *et al.*, 2008; Drouaud *et al.*, 2013). On the contrary, other proteins are known to inhibit crossover formation. In fact, *Arabidopsis msh2* mutants showed a significant 40% increase in crossover rates (Emmanuel *et al.*, 2006). Accordingly, using the previously described seed meiotic reporter line Col3-4/20 (Melamed-Bessudo *et al.*, 2005), we found that the rate of meiotic recombination was 97% higher in the *Arabidopsis msh7* mutants than in WT plants (Table 2). Although the magnitude of increase observed in our study is higher than previously reported for *Arabidopsis msh2* mutants, the use of a different tester line (Le5-11/22) and a different ecotype (Landsberg) may explain the difference. Our results strongly establish a role for AtMSH7 as a major meiotic anti-crossover factor, possibly in parallel to AtMSH2. Interestingly, the helicase Fanconi Anemia Complementation Group M (FANCM) was also described as another meiotic anti-crossover activity in *Arabidopsis* (Crismani *et al.*, 2012). This control of meiotic crossover formation has implications for plant breeding programmes since the number of crossovers is tightly constrained.

Taken together, results presented here indicate, for the first time, a differential expression of *MSH7* in actively dividing tissues, and the effect of the *MSH7* mutation on UV-B-induced DNA damage recognition and on the rates of somatic and meiotic recombination.

Supplementary material

Supplementary data can be found at *JXB* online.

Supplementary Table S1. List of PCR primers.

Supplementary Figure S1. Description of T-DNA lines. Exons are represented by black boxes, introns by thin black lines, and UTRs by white boxes. T-DNA insertions are indicated by triangles. Transcript levels were evaluated by qRT-PCR. Amplifications were performed using the primers shown in Supplementary Table S1.

Funding

This research was supported by grants from Agencia Nacional de Promoción Científica y Tecnológica (PICT 2012–267, PICT 2013-268, and PICT 2010–458 to PC and CPS) and Consejo Nacional de Investigaciones Científicas y Técnicas (CONICET; PIP 0018 to CPS). PC and CPS are members of the Researcher Career of CONICET.

Acknowledgements

We wish to thank José Manuel Pellegrino for technical assistance with microscopic analysis, Juliana Martin for selecting some of the transgenic seeds, Cathy Melamed-Bessudo and Avraham Levy for providing the reporter lines, and the Arabidopsis Biological Resource Center (ABRC, Columbus, OH, USA) for providing mutant seed stocks.

References

Acharya S, Wilson T, Gradia S, Kane MF, Guerrette S, Marsischky GT, Kolodner R, Fishel R. 1996. hMSH2 forms specific mispair-binding complexes with hMSH3 and hMSH6. *Proceedings of the National Academy of Sciences, USA* **93,** 13629–13634.

Ade J, Belzile F, Philippe H, Doutriaux M. 1999. Four mismatch repair paralogues coexist in *Arabidopsis thaliana*: AtMSH2, AtMSH3, AtMSH6-1 and AtMSH6-2. *Molecular and General Genetics* **262,** 239–249.

Alonso J, Stepanova A, Leisse T *et al.* 2003. Genome-wide insertional mutagenesis of *Arabidopsis thaliana*. *Science* **301,** 653–657.

Caryl A, Jones G, Franklin F. 2003. Dissecting plant meiosis using *Arabidopsis thaliana* mutants. *Journal of Experimental Botany* **54,** 25–38.

Clough SJ, Bent AF. 1998. Floral dip: a simplified method for *Agrobacterium*-mediated transformation of *Arabidopsis thaliana*. *The Plant Journal* **16,** 735–743.

Crismani W, Girard C, Froger N, Pradillo M, Santos JL, Chelysheva L, Copenhaver GP, Horlow C, Mercier R. 2012. FANCM limits meiotic crossovers. *Science* **336,** 1588–1590.

Culligan K, Hays J. 2000. *Arabidopsis* MutS homologs-AtMSH2, AtMSH3, AtMSH6, and a novel AtMSH7-form three distinct protein heterodimers with different specificities for mismatched DNA. *The Plant Cell* **12,** 991–1002.

Dion E, Li L, Jean M, Belzile F. 2007. An *Arabidopsis* MLH1 mutant exhibits reproductive defects and reveals a dual role for this gene in mitotic recombination. *The Plant Journal* **51,** 431–440.

Dong C, Whitford R, Langridge P. 2002. A DNA mismatch repair gene links to the *Ph2* locus in wheat. *Genome* **45,** 116–124.

Donnelly P, Bonetta D, Tsukaya H, Dengler R, Dengler N. 1999. Cell cycling and cell enlargement in developing leaves of *Arabidopsis*. *Developmental Biology* **215,** 407–419.

Drouaud J, Khademian H, Giraut L, Zanni V, Bellalou S, Henderson I, Falque M, Mézard C. 2013. Contrasted patterns of crossover and non-crossover at *Arabidopsis thaliana* meiotic recombination hotspots. *PLoS Genetics* **9,** e1003922.

Durant S, Paffett K, Shrivastav M, Timmins G, Morgan W, Nickoloff J. 2006. UV radiation induces delayed hyperrecombination associated with hypermutation in human cells. *Molecular and Cellular Biology* **26,** 6047–6055.

Emmanuel E, Yehuda E, Melamed-Bessudo C, Avivi-Ragolsky N, Levy AA. 2006. The role of *AtMSH2* in homologous recombination in *Arabidopsis thaliana*. *EMBO Reports* **7,** 100–105.

Genschel J, Littman S, Drummond J, Modrich P. 1998. Isolation of MutSβ from human cells and comparison of the mismatch repair specificities of MutSβ and MutSα. *The Journal of Biological Chemistry* **273,** 19895–19901.

Gomez RL, Spampinato CP. 2013. Mismatch recognition function of *Arabidopsis thaliana* MutSγ. *DNA Repair* **12,** 257–264.

Higgins J, Armstrong S, Franklin F, Jones G. 2004. The *Arabidopsis* MutS homolog *AtMSH4* functions at an early step in recombination: evidence for two classes of recombination in *Arabidopsis*. *Genes and Development* **18,** 2557–2570.

Higgins J, Vignard J, Mercier R, Pugh A, Franklin F, Jones G. 2008. AtMSH5 partners AtMSH4 in the class I meiotic crossover pathway in *Arabidopsis thaliana*, but is not required for synapsis. *The Plant Journal* **55,** 28–39.

Hoffmann E, Borts R. 2004. Meiotic recombination intermediates and mismatch repair proteins. *Cytogenetic and Genome Research* **107,** 232–248.

Hoffman P, Leonard J, Lindberg G, Bollmann S, Hays J. 2004. Rapid accumulation of mutations during seed-to-seed propagation of mismatch-repair-defective *Arabidopsis*. *Genes and Development* **18,** 2676–2685.

Horwath M, Kramer W, Kunze R. 2002. Structure and expression of the *Zea mays* mutS-homologs *Mus1* and *Mus2*. *Theoretical and Applied Genetics* **105,** 423–430.

Hsieh P, Yamane K. 2008. DNA mismatch repair: Molecular mechanism, cancer, and ageing. *Mechanisms of Ageing and Development* **129,** 391–407.

Iyer R, Pluciennik A, Burdett V, Modrich P. 2006. DNA mismatch repair: functions and mechanisms. *Chemical Reviews* **106,** 302–323.

Jefferson RA. 1987. Assaying chimeric genes in plants: the GUS gene fusion system. *Plant Molecular Biology Reporter* **5,** 387–405.

Jiricny J. 2006. The multifaceted mismatch-repair system. *Nature Reviews Molecular Cell Biology* **7,** 335–346.

Kunkel T, Erie D. 2005. DNA mismatch repair. *Annual Review of Biochemistry* **74,** 681–710.

Lafleuriel J, Degroote F, Depeiges A, Picard G. 2007. Impact of the loss of AtMSH2 on double-strand break-induced recombination between highly diverged homeologous sequences in *Arabidopsis thaliana* germinal tissues. *Plant Molecular Biology* **63,** 833–846.

Lario LD, Ramirez-Parra E, Gutierrez C, Casati P, Spampinato CP. 2011. Regulation of plant *MSH2* and *MSH6* genes in the UV-B-induced DNA damage response. *Journal of Experimental Botany* **62,** 2925–2937.

Li G-M. 2008. Mechanisms and functions of DNA mismatch repair. *Cell Research* **18,** 85–98.

Li L, Dion E, Richard G, Domingue O, Jean M, Belzile FJ. 2009. The *Arabidopsis* DNA mismatch repair gene *PMS1* restricts somatic recombination between homeologous sequences. *Plant Molecular Biology* **69,** 675–684.

Li L, Jean M, Belzile F. 2006. The impact of sequence divergence and DNA mismatch repair on homeologous recombination in *Arabidopsis*. *The Plant Journal* **45,** 908–916.

Li L, Santerre-Ayotte S, Boivin EB, Jean M, Belzile F. 2004. A novel reporter for intrachromosomal homoeologous recombination in *Arabidopsis thaliana*. *The Plant Journal* **40,** 1007–1015.

Lloyd AH, Milligan AS, Langridge P, Able JA. 2007. *TaMSH7*: A cereal mismatch repair gene that affects fertility in transgenic barley (*Hordeum vulgare* L.). *BMC Plant Biology* **7,** 67.

Melamed-Bessudo C, Levy A. 2012. Deficiency in DNA methylation increases meiotic crossover rates in euchromatic but not in heterochromatic regions in *Arabidopsis*. *Proceedings of the National Academy of Sciences, USA* **109,** E981–E988.

Melamed-Bessudo C, Yehuda E, Stuitje A, Levy A. 2005. A new seed-based assay for meiotic recombination in *Arabidopsis thaliana*. *The Plant Journal* **43,** 458–466.

Opperman R, Emmanuel E, Levy A. 2004. The effect of sequence divergence on recombination between direct repeats in *Arabidopsis*. *Genetics* **168,** 2207–2215.

Osman K, Higgins J, Sanchez-Moran E, Armstrong S, Franklin F. 2011. Pathways to meiotic recombination in *Arabidopsis thaliana*. *New Phytologist* **190,** 523–544.

Pecinka A, Fang W, Rehmsmeier M, Levy A, Mittelsten Scheid O. 2011. Polyploidization increases meiotic recombination frequency in *Arabidopsis*. *BMC Biology* **9,** 24.

Pfeifer G, You Y, Besaratinia A. 2005. Mutations induced by ultraviolet light. *Mutation Research* **571,** 19–31.

Ries G, Buchholz G, Frohnmeyer H, Hohn B. 2000*a*. UV-damage-mediated induction of homologous recombination in *Arabidopsis* is dependent on photosynthetically active radiation. *Proceedings of the National Academy of Sciences, USA* **97,** 13425–13429.

Ries G, Heller W, Puchta H, Sandermann H, Seidlitz H, Hohn B. 2000*b*. Elevated UV-B radiation reduces genome stability in plants. *Nature* **406,** 98–101.

Sambrook J, Russel DW. 2001. *Molecular cloning – a laboratory manual*. Cold Spring Harbor: Cold Spring Harbor Laboratory Press.

Spampinato CP, Gomez RL, Galles C, Lario LD. 2009. From bacteria to plants: a compendium of mismatch repair assays. *Mutation Research* **682,** 110–128.

Stapleton AE, Mori T, Walbot V. 1993. A simple and sensitive antibody-based method to measure UV-induced DNA damage in *Zea mays*. *Plant Molecular Biology Reporter* **11,** 230–236.

Tam S, Hays J, Chetelat R. 2011. Effects of suppressing the DNA mismatch repair system on homeologous recombination in tomato. *Theoretical and Applied Genetics* **123,** 1445–1458.

Tam SM, Samipak S, Britt A, Chetelat RT. 2009. Characterization and comparative sequence analysis of the DNA mismatch repair *MSH2* and *MSH7* genes from tomato. *Genetica* **137,** 1–14.

Wu S-Y, Culligan K, Lamers M, Hays J. 2003. Dissimilar mispair-recognition spectra of *Arabidopsis* DNA-mismatch-repair proteins MSH2*MSH6 (MutSα) and MSH2*MSH7 (MutSγ). *Nucleic Acids Research* **31,** 6027–6034.

Youds J, Boulton S. 2011. The choice in meiosis - defining the factors that influence crossover or non-crossover formation. *Journal of Cell Science* **124,** 501–513.